CHARACTERIZATION OF BENDING FRACTURE OF STRESS BIASED PIEZOELECTRIC COMPOSITE ACTUATORS BY ACOUSTIC EMISSION

Sung-Choong Woo[1], Nam Seo Goo[2]

[1]Artifcial Muscle Research Center, Konkuk University, Seoul, South Korea
[2]Intelligent Microsystem Program, Department of Advanced Technology Fusion, Konkuk University, Seoul, South Korea

Abstract

In this work, the bending fracture process of a stress biased piezoelectric composite actuator (PCA) under a three-point bending load have been characterized with the aid of acoustic emission (AE) monitoring. The AE signal from the monolithic PZT wafer at the maximum bending load shows the characteristics of high amplitude and long duration with a low dominant frequency band confirmed by a fast Fourier transform. For PCAs, the AE signals emitted in stage II have amplitude higher than 80 dB and a low dominant frequency band characteristic. Such signals are due to the brittle fracturing in the PZT layer and/or the growth of delamination between the PZT and the fiber composite layers. The signals with high amplitude and a high dominant frequency band in stage III generate by the fiber breakages hindering the main crack propagation in the glass bottom layer along with the macro-delamination between the PZT layer and the fiber composite layer. Based on the AE analysis and fracture observations, the bending fracture process of stress-biased PCAs has been reasonably characterized.

1. Introduction

Piezoelectric actuators, which are being applied to shape and vibration controllers in the field of lightweight aerospace, show an outstanding actuating performance and have a great potential for a variety of applications [1-6]. More recently, research has been conducted on micro-pump based on MEMS technology for drug delivery applications in the medical industry and on synthetic jet actuators that control the stall induced by air separation on the wing surface [7,8]. However, piezoelectric actuators that consist of thin metal layers or fiber composite layers bonded to thin PZT plate show a weakness against the delamination between the PZT layer and metal or fiber composite layers; they also show a weakness with respect to the residual stresses induced by differences in the thermal contraction of PZT and fiber composite layers during the manufacturing process. Although one kind of piezoelectric actuator is commercially available under the trade name of THUNDER [2], there has been little verification of the damage characteristics and integrity of the piezoelectric actuators that have been developed. Conventional studies concerning piezoelectric actuators have concentrated on enhancing the actuating displacement or the actuating load capabilities.

[1]lilsuzy@hanyang.ac.kr
[2]nsgoo@konkuk.ac.kr

In addition, because the main actuating mode of piezoelectric actuators is the bending mode, we need to study the damage process and the failure mechanism of piezoelectric actuators under a bending load in order to ensure their safety, integrity and reliability.

An acoustic emission (AE) monitoring, on the other hand, is sometimes used for nondestructive inspections of the status of deformation and fractures in various engineering materials, such as metals, fiber-reinforced plastics, metal matrix composites and hybrid laminates [9-17]. Thus, to understand damage processes in piezoelectric actuators using AE monitoring, AE characteristics of the constituent layers of monolithic PZT and fiber composites should be considered simultaneously. Such consideration is important because the fracture mechanisms of piezoelectric composite actuators include brittle fracturing of the PZT ceramic layer, delamination between the PZT and fiber composite layers, as well as matrix cracking and fiber breakage in the fiber composite layer. In previous studies [18,19], the present authors have analyzed a stress biased Piezoelectric Composite Actuator (PCA) via three-dimensional finite element simulations considering the thermal deformation which occurred in each layer during the curing process and we experimentally investigated how the PZT thickness, the lay-up sequence, the boundary condition, the applied electric field and

the drive frequency affected the performance of the PCA.

In the present work, we focus on the characterization of the bending fracture process of stress biased PCAs. To achieve this goal, we used an AE parametric approach using event rate, amplitude and duration. We also analyze the dominant frequency bands with the aid of a fast Fourier transform (FFT). After the bending test, fracture observations are conducted with optical microscopy and scanning electron microscopy to examine the fracture mechanisms of a PCA.

2. Experimental

2.1. Actuating principle of a PCA

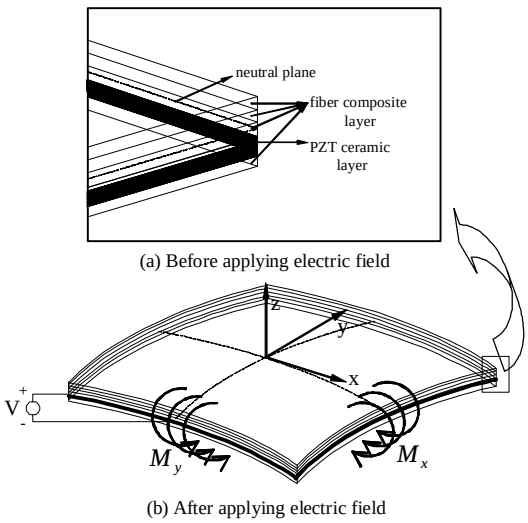

Figure 1*: The actuating principle of a stress biased piezoelectric composite actuator.*

Fig. 1 shows the actuating principle of a PCA. The polling direction of the PZT ceramic is along the z-axis. When a high voltage is applied to the commercially poled PZT plate, a polarizing phenomenon takes place in the PZT layer and then the PZT tends to contract due to the negative piezoelectric strain constant of d_{31}. At this time, if a neutral plane by moment equilibrium exists outside the PZT layer, the PZT ceramic deforms in-plane direction; thus, an asymmetrically laminated plate with PZT wafer has bending deformation. If a PCA is symmetrically laminated and PZT is embedded in the middle of the laminate, the PCA does not bend.

2.2. Materials

To fabricate PCAs, we used carbon-epoxy prepreg (WSN1K-B, SK Chemicals), glass-epoxy prepreg (GEP108, SK Chemicals) and a commercially poled PZT ceramic (3203HD, CTS Co.). Their thicknesses are 0.105 mm, 0.07 mm and 0.25 mm respectively. Woven fabric carbon- and glass-epoxy prepregs were selected to avoid an anticlastic curvature during the curing process. To prevent short circuiting in applying electric field to the PCAs, we used carbon-epoxy prepregs that were smaller than the monolithic PZT in the hand lay-up procedure. In addition, to manufacture the clamping tab for the actuating test, we chose glass-epoxy prepregs that were longer and wider than the monolithic PZT. The bottom insulating layer of glass-epoxy plays a protective role the brittle PZT ceramic against the external environment. The actuator panels were co-cured in an autoclave for three hours at a temperature of 177℃ in accordance with the thermal cycle. Two types of PCAs with different lay-up configurations were used in this study: PCA-A and PCA-B. Fig. 2 presents the lay-up configuration and detailed manufacturing dimensions of the PCA, along with a photograph of the fabricated PCA-A.

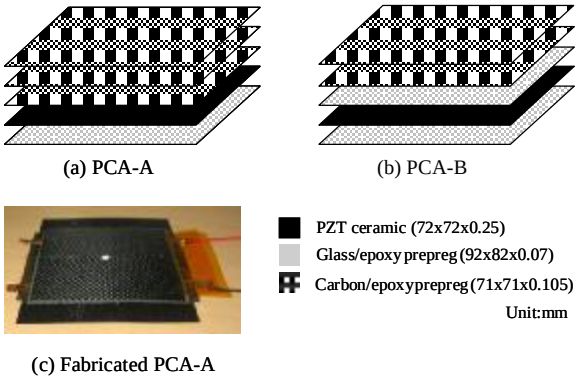

Figure 2*: Lay-up configuration of (a) the PCA-A and (b) the PCA-B; (c) a photograph of the fabricated PCA-A.*

2.3. Acoustic emission acquisition and three-point bending tests

Fig. 3 illustrates the AE measurement system and a three-point bending test. We used a one-channel AE detection system (MISTRAS 2001, PAC) to record the AE data in real time. The AE signals were detected by a resonant-type sensor (micro30, PAC) which had a bandwidth of 100 kHz to 600 kHz with a dominant sensitivity at 265 kHz. We used vacuum grease as a couplant to mount an AE sensor on one side of the PCA. We then adopted AE measurement conditions of 40 dB for the preamplifier, 40 dB for the system threshold, and 4 MHz for the sampling rate. Next, for the AE parametric analysis, we filtered the mechanical and electrical noises that had

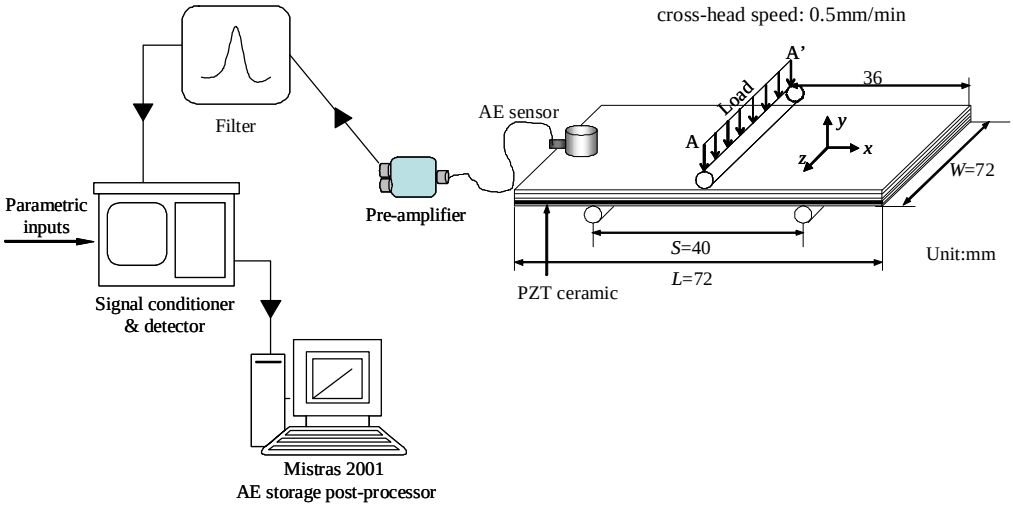

Figure 3*: Experimental set-up for a three-point bending test and an AE data acquisition.*

signals lasting less than 25 μs [13]. As illustrated in Fig. 3, we placed the monolithic PZT and the fabricated PCA on two fixed roller supports that were separated by a distance of 40 mm. Finally, we conducted a bending test using universal test machine (Zwick 250, testXpert) on the PCA with a cross-head speed of 0.5 mm/min. The load versus displacement curve was recorded. At the same time, damage onset and accumulation were monitored using AE measurement system. The bending load was applied by another roller with a diameter of 3.2 mm at a position of A–A' until the final failure of the PCA. After the bending test, we used optical microscopy (Camscope, Sometech Co.) and scanning electron microscopy (JSM-6380, JEOL Co.) to examine the damage state of PCAs.

3. Results and discussion

3.1. AE response of monolithic PZT according to bending fracture process

Fig. 4 shows a typical load-deflection (P-δ) curve and AE signals from monolithic PZT. From the P-δ curve, monolithic PZT exhibits typically brittle behavior: as the deflection increases, the load increases almost linearly to the maximum bending load (P_{max}). A catastrophic and abrupt fracture occurs at a deflection of 0.79 mm, which corresponds to P_{max} of 4.76 N. An AE signal emitted at P_{max} has the amplitude of 88 dB and the duration of 8.6 ms. The AE event with such high amplitude and long duration is generally associated with the propagation of macro-cracking and/or delamination in a high load level approaching the final failure [15,16]. The AE signals emitted after P_{max} show the characteristics of low amplitude (42 dB to 52 dB) and a short duration (less than 0.7 ms). These signals may be due to intergranular

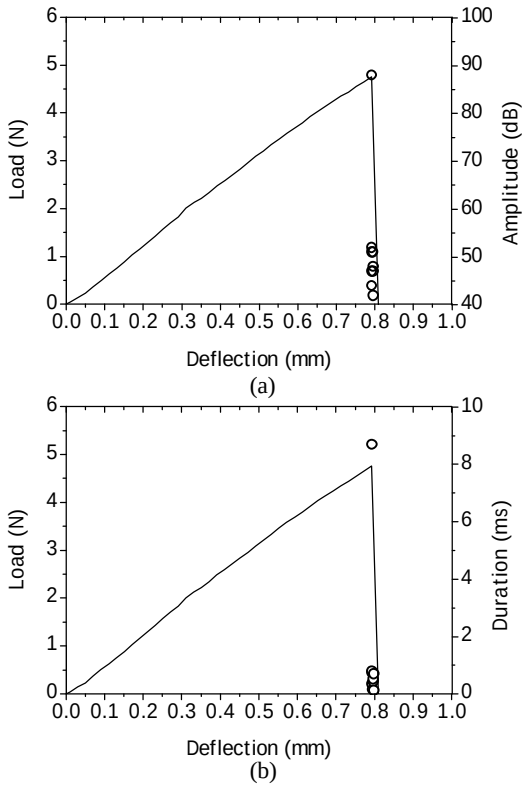

Figure 4*: AE signals from monolithic PZT ceramic: (a) a typical load-deflection curve and AE amplitude distribution; (b) a load-deflection curve and the distribution of duration.*

micro-damages during the very short period after P_{max}.

Fig. 5 shows typical FFT results of AE signals from monolithic PZT. Depending on the dominant frequency band and the magnitude in the power spectrum, the AE characteristics of monolithic PZT ceramic can be divided into two types. In the figure,

a dominant frequency band is defined as a band between the first peak frequency, which has

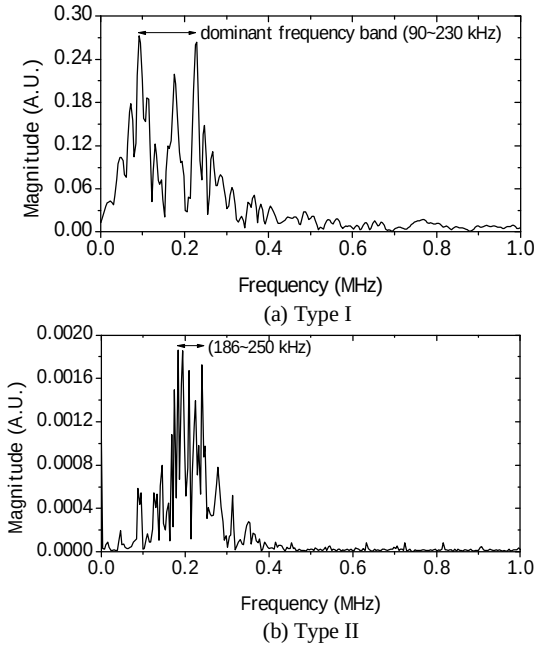

Figure 5*: Typical FFT results of an AE signal from PZT ceramic: (a) at P_{max} and (b) after P_{max}.*

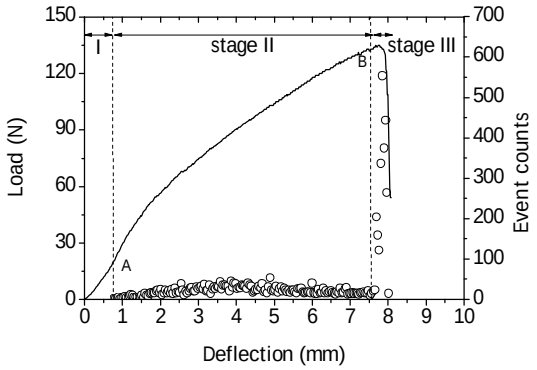

Figure 6*: A load-deflection curve and the corresponding behavior of AE counts for the PCA-A under a bending load.*

the highest magnitude in the spectrum, and the third peak frequency. As shown in Fig. 5(a), the type I signal at P_{max} has a low dominant frequency band of 90 kHz to 230 kHz and a high value in its magnitude. In contrast, the AE signals generated after P_{max} have a similar dominant frequency band of 186 kHz to 250 kHz but a low value in magnitude (type II) as compared with Fig. 5(a). The magnitude of signals from the monolithic PZT is different, but the dominant frequencies have a similar band. Thus, based on the dominant frequency band and amplitude, the AE characteristics of the monolithic PZT ceramic can be differentiated as a macro-fracture mode of catastrophic fracture at maximum bending load and a micro-fracture mode of intergranular micro-damage.

3.2. AE response of PCAs according to bending fracture process

Fig. 6 shows a typical P-δ curve and the corresponding behavior of the AE counts for PCA-A subjected to a bending load. In previous studies [18,19], the PCA-A had the best actuating performance under simply supported and fixed-free boundary conditions for a drive frequency of 1 Hz. From the P-δ curve and the AE event counts, the bending behavior of the PCA-A can be divided into three stages. In stage I (from the beginning to point A), we can see a linearity in the bending behavior and there are no detectable AE events, which indicates that any damage does not yet occur in the PCA-A. AE activities begins at around δ = 0.76 mm (point A) with a slight change in the slope of the P-δ curve, and at this time an audible fracture sound was released. In the case of laminated fiber composites, a damage initiation generally stems from the matrix part. The first AE burst at point A has amplitude of 85 dB, which is too high level to be considered generating from the matrix fracture according to Groot et al. [20] and is also similar to the AE characteristic of catastrophic fracturing from the monolithic PZT as shown in Fig. 4(a). In addition, deflection level at this time is nearly consistent with that of monolithic PZT except only that load level is different. Thus, it is concluded that the first AE burst in PCA-A must have originated from the brittle fracture in the PZT layer. Subsequently, the behavior of the AE count shows a gradual increase and then a slight decrease until δ = 7.6 mm (point B). Such AE behavior may suggest that a stable and continuous damage process occurs in the PZT layer.

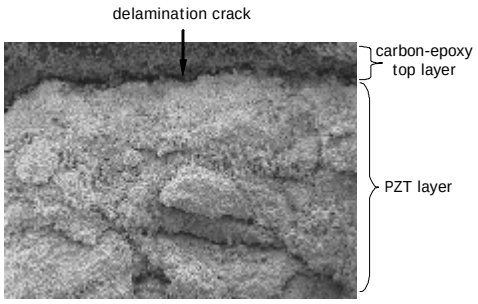

Figure 7*: Scanning electron micrograph of the fractured surface in PCA-A: delamination between the fiber-PZT interface layers and brittle fracture and cracks in the PZT layer*

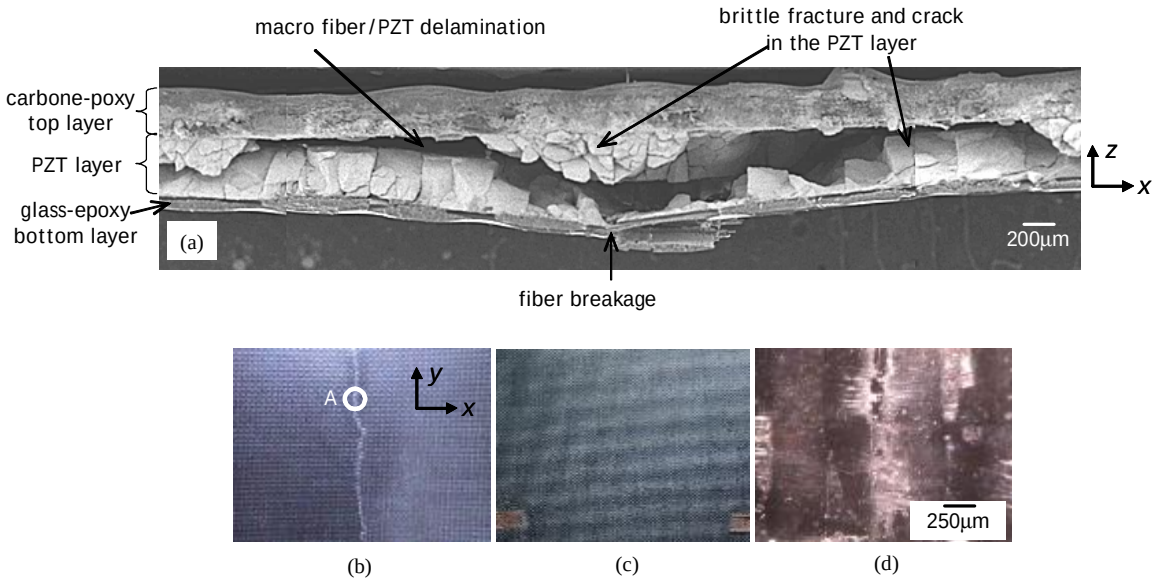

Figure 8*: Fractography : (a) various fracture mechanisms of the PCA-A, (b) the main cracking on the surface of glass-epoxy bottom layer; (c) no damage in the carbon-epoxy top layer;(d) an enlarged view of circle A in photo (b).*

Fig. 7 shows SEM photographs taken from the fracture surfaces of the PCA-A in stage II. As a bending load increase, a crack occurred early in the PZT layer propagates along the PZT-fiber composite interface layer, thereby inducing the delamination crack as shown in Fig. 7. At this time, the matrix fracture in the fiber layer is expected to happen during the delamination growth at the interface layer, generating both weak and strong emissions with a low AE event count. In stage III, a further increase and then a sharp load drop in the P-δ curve are observed. At the beginning of stage III (point B), the AE counts temporarily decrease to a minimum and then sharply increase in AE activity explaining the occurrence of a critical mode in the fiber breakage.

Final damage states of PCA-A after bending test are presented in Fig. 8(a) where we can see rough damage surfaces and large brittle fractures in the PZT layer, fiber breakages at the center portion in the glass bottom layer and the macro delamination between the PZT ceramic and fiber composite layers. Such complicated fracture process is evidently associated with aforementioned AE activity. In Fig. 8(b), a long and almost straight main cracking is obviously observed on the surface of glass-epoxy bottom layer. In Fig. 8(c), however, no crack and no damage are seen on the surface of carbon-epoxy top layer because of the high bending strength of the carbon-epoxy layer under the state of compressive stress. In Fig. 8(d), the enlarged views of a circle 'A' in photo (b), the fiber breakages and fiber-matrix debondings are much conspicuous. Considering that the used carbon and glass-epoxy resin prepregs are woven fabric fiber composite systems and the applied load is an out-of-plane bending load, such fracture mechanisms are reasonable.

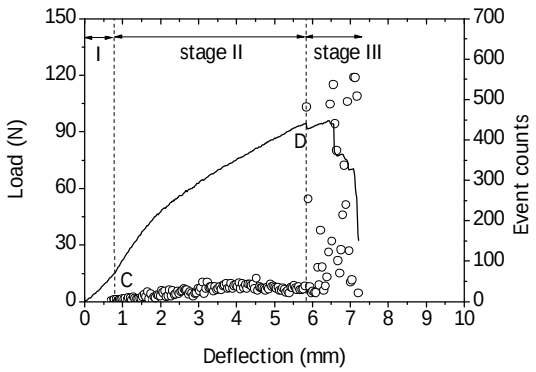

Figure 9*: A load-deflection curve and the corresponding behavior of AE counts for the PCA-B under a bending load.*

Fig. 9 shows a typical P-δ curve and the corresponding behavior of the AE event counts for PCA-B subjected to a bending load. Overall, the behavior of load and the corresponding AE activity are similar to those of PCA-A. The reasons for this is that the used fiber composites are a woven fabric system and the critical damage of fiber breakages happens only in the brittle PZT layer and the glass-epoxy bottom layer where highest tensile stresses are applied. If unidirectional fiber composite systems were used and a tensile load was applied to PCAs, their AE characteristics would be different.

Fig. 10 shows the distribution of the amplitude and duration of AE signals versus the test time for PCA-A and PCA-B. From the beginning of an event in PCA-A and PCA-B, many events higher

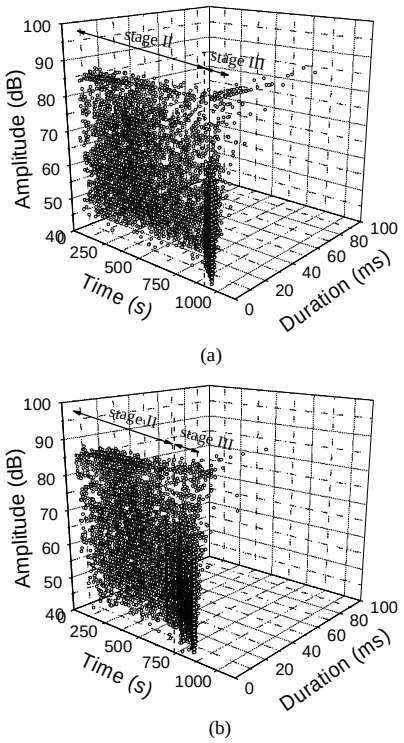

Figure 10*: Distribution of the AE amplitude and duration versus the test time for (a) PCA-A and (b) PCA-B.*

than 80 dB in amplitude are constantly generated throughout stage I. In the case of laminated composites, the initial damage generally originates with a matrix fracture and final fracture results from fiber breakages. According to the result of other researcher, the AE amplitude ranges are 30 dB to 60 dB for matrix cracking, 80 dB to 97 dB for fiber breakage, and 60 dB to 85 dB for interlaminar delamination [22]. Thus, most of the strong emissions with high amplitude and long duration in stage II may originate from brittle fractures in the PZT layer and from delamination near the interface layers of the PZT and the fiber composite rather than originating from fiber breakages. In stage III, many AE signals are generated with an amplitude higher than 87 dB and a duration longer than 5 ms. At this load stage, there must be various complex bending fracture process; for example, the crack initiation and the rapid propagation in the glass-epoxy bottom layer where the highest tensile stress is applied; the breakages of the bridged fibers that accompany the matrix cracks; and the delamination between the PZT ceramic and the adjacent fiber composite layers. Accordingly, we can use the AE characteristics to monitor the damage process in PCAs showing up multiple modes of damage.

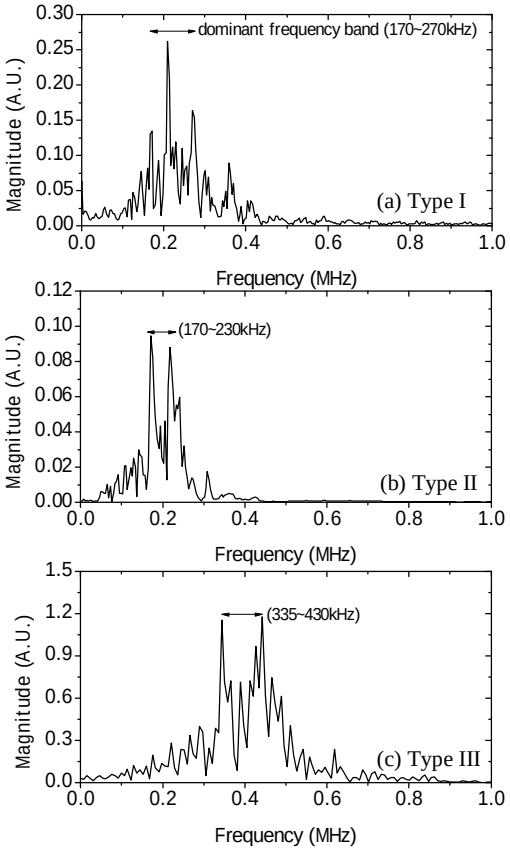

Figure 11*: FFT results for representative AE signals according to the fracture process: (a) a low dominant frequency band with a high magnitude, (b) a low dominant frequency band with a low magnitude and (c) a high dominant frequency band with a high magnitude.*

On the basis of the dominant frequency band and the magnitude in the spectrum, we classified the signals from PCAs into three types and representative results are presented in Fig. 11. The type I signal corresponding to the first event generated from the individual PCA shows a low dominant frequency band of 170 kHz to 270 kHz and a high magnitude in its value. It should be noted that characteristic of dominant frequency band of type I is analogous to that from the monolithic PZT at the maximum bending load as shown in Fig. 5(a). Hence, such a type of signal must have originated from the brittle fracture in the PZT core layer. The type II signal, which is a representative of the frequency distribution in stage II, reveals the band of a low dominant frequency in a range of 170 kHz to 230 kHz. In comparison with type I, type II has a similar dominant frequency band but has a lower value in magnitude indicating that each source of

emission is different. On this point, it is notable that type I signals were detected along with type II signals at a constant rate for the entirety of stage II and III. If

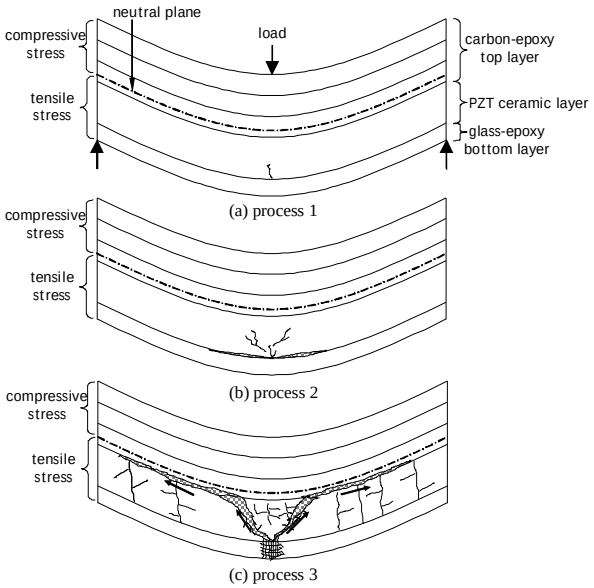

Figure 12*: The bending fracture process of crack propagation and delamination growth in the PCA-A subjected to a bending load.*

the type I is actually caused by the brittle fracture in the PZT layer, type II can be expected to be due to matrix deformation, fiber-matrix debonding as well as micro delamination at the fiber-PZT interface layer. On the other hand, type III signal whose amplitude is higher than 70dB mainly occurring in stage III is different from type I and II in that it has a higher dominant frequency band of 335 kHz to 430 kHz than type I and type II and its magnitude is 3 to 30 times higher than that of type I and type II. Therefore, such signals as type III is evidently due to the fiber breakages during the main crack propagation in the glass bottom layer and macro PZT-fiber interface delamination. Hence, the bending fracture process of PCAs can be differentiated and described from the dominant frequency band and the magnitude in spectrum.

3.3. Modeling of damage processes in association with AE characteristics

Based on the aforementioned AE behavior combined with fracture observations, the damage evolution for the PCA-A during the bending fracture process is schematically illustrated in Fig. 12. The dash-dot lines in the figure indicate neutral planes by moment equilibrium obtained by using the classical lamination theory. There are three processes in the overall bending fracture for PCAs. As an applied bending load increases, in process 1, damage initiates emitting AE signals of a low dominant frequency band with a high magnitude (type I) in the brittle PZT ceramic layer rather than in the flexible glass-epoxy bottom layer. In process 2, the micro cracks in the PZT core layer propagate along the interface between PZT ceramic and fiber composite layers resulting in a local delamination, and then the local delamination grows along the interface layers generating strong and weak emissions such as type I and II signals. While the damage evolutions continue throughout the entirety of stage II, small amount of fiber breakage together with fiber-matrix debondings takes place generating the small number of signals (type III). In process 3, just prior to the maximum bending load, the main cracking caused by fiber breakages in the glass-epoxy bottom layer induces the macro delamination between the PZT and the fiber layers. During this process, many strong emissions with a high dominant frequency band and a high magnitude (type III) are released. Judging from that the AE characteristics of individual PCAs are similar to each other, it is believed that the bending fracture process for PCA-A is not different from PCA-B.

4. Conclusions

In this work, we characterized the bending fracture of stress biased piezoelectric composite actuators under three-point bending loads with the aid of acoustic emission technique. We also examined the failure mechanism of PCAs by means of transmission optical microscopy and scanning electron microscopy. Our conclusions from the study are as follows:

i) The AE characteristics of a catastrophic fracture in the PZT ceramic plate at the maximum bending load revealed amplitude higher than 80 dB and duration longer than 8 ms. The frequency characteristic through the FFT showed a low dominant frequency band with a high magnitude in the spectrum.

ii) The first AE event from PCAs under a bending load generated from the brittle fracture in the PZT layer, which was explained by the above mentioned AE characteristics of PZT ceramic. The AE signals having a low dominant frequency band with high amplitude and a long duration in stage I were generated not by the fiber breakages but by the brittle fracture in the PZT layer and the growth of local delamination between the PZT and the fiber composite layers. Thus, the dominant frequency characteristics combined with such AE parameters

as event rate, amplitude and duration can be used to describe the damage processes of a PCA subjected to a bending load.

iii) The fracture processes of PCAs with thin PZT ceramic plate include brittle fracturing in the PZT layer, matrix cracking and fiber breakage in the fiber composite layer, as well as delamination between the PZT and the fiber composite layers, which were successfully monitored during the AE measurement. Hence, an AE monitoring is an informative and powerful tool for identifying the damage processes in a PCA.

5. Acknowledgement

The present work was supported by the Korea Research Foundation Grant (KRF-2004-005-D00045/D00046). The authors appreciate this financial support.

6. References

[1] Haertling, G.H., "Rainbow ceramics - a new type of ultra-high-displacement actuator", *Bull. Am. Ceram. Soc.*, 73:93-96, 1994.

[2] Hellbaum, R., Bryant, R. and Fox, R., "Thin layer composite unimorph ferroelectric driver and sensor", *US patent*, No. 5632841, 1997.

[3] Andy, H., Goo, N.S., Park, K.C. and Yoon, K.J., "Modeling and analysis for the development of Lightweight Piezoceramic Composite Actuators (LIPCA)", *Compu. Mater. Sci.*, 30:474-481, 2004.

[4] Kim, K.Y., Park, K.H., Park, H.C., Goo, N.S. and Yoon, K.J., "Performance evaluation Lightweight piezo-composite actuator", *Sens. Actua. A*, 120:123-129, 2005.

[5] Yoon, K.J., Park, K.H., Lee, S.K., Goo, N.S. and Park, H.C., "Analytical design model for a piezo-composite unimorph actuator and its verification using lightweight piezo-composite curved actuators", *Smart Mater. Struc.*, 13:459-467, 2004.

[6] Lynch, C.S., "Low frequency bending piezoelectric actuator with integrated ultrasonic NDE functionality", *NDT&E Int.*, 38:627-633, 2005.

[7] Teymoori, M. and Ebrahim, A., "Design and simulation of a novel electrostatic peristaltic micromachined pump for drug delivery applications", *Sens. Actua. A*, 117:222-229, 2005.

[8] Liang, Y., Kuga, Y. and Taya, M., "Design of membrane actuator based on ferromagnetic shape memory alloy composite for synthetic jet applications", *Sens. Actua A*, 121:1-7, 2005.

[9] Gang, Q., "Wavelet-based AE characterization of composite materials", *NDT&E Int.*, 33:133-144, 2000.

[10] Velayudham, A., Krishnamurthy, R. and Soundarapandian, T., "Acoustic emission based drill condition monitoring during drilling of glass/phenolic polymeric composite using wavelet packet transform", *Mater. Sci. & Eng. A*, 412:141-145, 2005.

[11] Máthis, K., Chmelík, F., Trojanová, Z., Luká P. and Lendvai, J., "Investigation of some magnesium alloys by use of the acoustic emission technique", *Mater. Sci. & Eng. A*, 387:331-335, 2004.

[12] Kim, S.T. and Lee, Y.T, "Characteristics of damage and fracture process of carbon fiber reinforced plastic under loading-unloading test by using AE method", *Mater. Sci. & Eng. A*, 234-236:322-326, 1997.

[13] Choi, N.S., Takahashi, K. and Hoshino, K., "Characteristics of acoustic emission during the damage process in notched short-fibre-reinforced thermoplastics", *NDT&E Int.*, 25:271-278, 1992.

[14] Woo, S.C. and Choi, N.S., "Analysis of fracture process in single-edge-notched laminated composites based on the high amplitude acoustic emission events", *Compos. Sci. Tech.*, (in press)

[15] Woo, S.C. and Choi, N.S., "Analysis of dominant frequencies of glass fiber/aluminum laminates during acoustic emission measurement", *Key Eng. Mater.*, 321:901-906, 2006.

[16] Woo, S.C. and Choi, N.S., "Analysis of dominant frequencies of glass fiber/aluminum laminates during acoustic emission measurement", *Key Eng. Mater.*, 321:901-906, 2006.

[17] Rabiei, A., Enoki, M. and Kishi, T., "A study on fracture behavior of particle reinforced metal matrix composites by using acoustic emission source characterization", *Mater. Sci. & Eng. A*, 293:81-87, 2000.

[18] Woo, S.C. and Goo, N.S., "Analysis of a Plate-type Piezoelectric Composite Unimorph Actuator Considering Thermal Residual Deformation", *Trans. of KSME (in Korean)*, 30(4):409-419, 2006.

[19] Woo, S.C. and Goo, N.S., "Bending characteristics of plate-type piezoelectric composite actuators according to applied electric fields and drive frequencies", *Key Eng. Mater.*, 326:1701-1704, 2006.

[20] De groot, P., Wijnen, P. and Janssen, R., "Real-time frequency determination of acoustic emission for different fracture mechanisms in carbon/epoxy composites", *Compos. Sci. Tech.*, 55:405-12,1995.

[21] Benmedakhene, S., Kenane, M. and Benzeggagh, M.L., "Initiation and growth of delamination in glass/epoxy composites subjected to static and dynamic loading by acoustic emission monitoring", *Compos. Sci. Tech.*, 59:201-208, 1999.

[22] Zhuang, X. and Yan, X., "Investigation of damage mechanisms in self-reinforced polyethylene composites by acoustic emission", *Compos. Sci. Tech.*, 66:444-449, 2006.